Supplementary Material

Facile photogeneration of a charge separated state in a cyanoacetylide bridged Fe(II)-Re(I) heterobimetallic complex.

Mark E. Smith,[†] Emma L. Flynn,[†] Mark A. Fox,[†] Alexandre Trottier,[†] Eckart Wrede,[†] Dmitri S. Yufit,[†] Judith A.K. Howard,[†] Kate L. Ronayne,[‡] Michael Towrie,[‡] Anthony W. Parker,[‡] František Hartl*[,⊥] and Paul J. Low*[,†]

Department of Chemistry, Durham University, South Rd, Durham, DH1 3LE, UK

Central Laser Facility, STFC Rutherford Appleton Laboratory, Chilton, Didcot, Oxfordshire, OX11 0QX, UK

Van 't Hoff Institute for Molecular Sciences, University of Amsterdam, Nieuwe Achtergracht 166, 1018 WV Amsterdam, The Netherlands

Contents

Figure S1 The cyclic voltammogram of [**3**]PF_6 (0.1 M NBu_4PF_6 / thf, –50°C).[a]

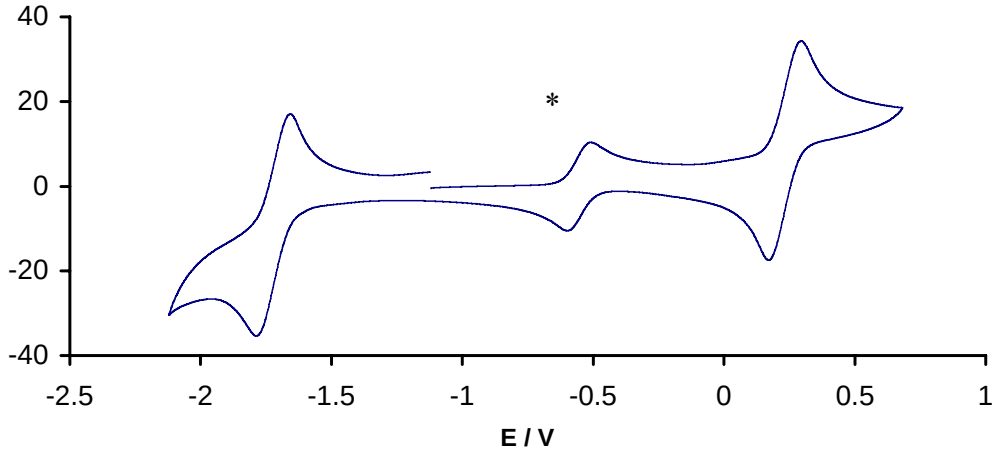

* Decamethylferrocene internal reference, –0.56 V vs ferrocene.

Computational details

All computations were carried out with the Gaussian 03 package[1] using models which employ a $Fe(dHpe)_2Cp$ fragment rather than the Fe(dppe)Cp moiety to reduce computational effort, for the experimental geometries **[3]$^{n+}$** (n = 0, 1, 2) and are denoted **[3-H]$^{n+}$**. The model geometries of the bimetallic species, **[3-H]$^{n+}$** (n = 0, 1, 2), were optimized using the PBE1PBE[2] functionals with no symmetry constraints using the 6-31G* [3] basis set for the O atoms and the pseudopotentials LANL2DZ[4] for all other atoms. Frequencies were calculated on these optimized geometries. No imaginary frequencies were obtained which indicates that the computed geometries are true minima of the potential energy surface. A scaling factor of 0.95 was applied to the calculated IR frequencies.[5] Small energy differences were found between geometries where the metal fragments in **[3-H]$^{n+}$** (n = 0, 1, 2) are disposed in either a *cisoid* and *transoid* fashion, and indeed both conformations are found as true minima. The more stable *cisoid* forms of **[3-H]$^{n+}$** (n = 0, 1, 2) geometries have total energy values of -1492.86858, -1492.71820 and -1492.40561 hartrees respectively whereas the *transoid* forms have corresponding values of -1492.86352, -1492.71615 and -1492.40373 hartrees. The *cisoid* conformations of **[3-H]$^{n+}$** (n = 0, 1, 2) are examined in detail here. Electronic structure calculations and TD-DFT calculations were also carried out at the same level of theory.

---

1. Gaussian 03, Revision C.02, Frisch, M.J.; Trucks, G.W.; Schlegel, H.B.; Scuseria, G.E.; Robb, M.A.; Cheeseman, J.R.; Montgomery, Jr., J.A.; Vreven, T.; Kudin, K.N.; Burant, J.C.; Millam, J.M.; Iyengar, S.S.; Tomasi, J.; Barone, V.; Mennucci, B.; Cossi, M.; Scalmani, G.; Rega, N.; Petersson, G.A.; Nakatsuji, H.; Hada, M.; Ehara, M.; Toyota, K.; Fukuda, R.; Hasegawa, J.; Ishida, M.; Nakajima, T.; Honda, Y.; Kitao, O.; Nakai, H.; Klene, M.; Li, X.; Knox, J.E.; Hratchian, H.P.; Cross, J.B.; Adamo, C.; Jaramillo, J.; Gomperts, R.; Stratmann, R.E.; Yazyev, O.; Austin, A.J.; Cammi, R.; Pomelli, C.; Ochterski, J.W.; Ayala, P.Y.; Morokuma, K.; Voth, G.A.; Salvador, P.; Dannenberg, J.J.; Zakrzewski, V.G.; Dapprich, S.; Daniels, A.D.; Strain, M.C.; Farkas, O.; Malick, D.K.; Rabuck, A.D.; Raghavachari, K.; Foresman, J.B.; Ortiz, J.V.; Cui, Q.; Baboul, A.G.; Clifford, S.; Cioslowski, J.; Stefanov, B.B.; Liu, G.; Liashenko, A.; Piskorz, P.; Komaromi, I.; Martin, R.L.; Fox, D.J.; Keith, T.; Al-Laham, M.A.; Peng, C.Y.; Nanayakkara, A.; Challacombe, M.; Gill, P.M.W.; Johnson, B.; Chen, W.; Wong, M.W.; Gonzalez, C.; Pople, J.A. Gaussian, Inc., Wallingford CT, 2004.
2. Perdew, J.P.; Burke, K.; Ernzerhof, M. *Phys. Rev. Lett.* **1996**, *77*, 3865.
3. (a) Petersson G.A.; Al-Laham, M.A. *J. Chem. Phys.* **1991**, *94*, 6081. (b) Petersson, G.A.; Bennett, A.; Tensfeldt, T.G.; Al-Laham, M.A.; Shirley, W.A.; Mantzaris, J. *J. Chem. Phys.* **1988**, *89*, 2193.
4. (a) Dunning Jr., T.H.; P. J. Hay, in *Modern Theoretical Chemistry*, Ed. H. F. Schaefer III, Vol. 3 (Plenum, New York, 1976). (b) Hay, P.J.; Wadt, W.R. *J. Chem. Phys.* **1985**, *82*, 270. (c) Wadt, W.R.; Hay, P.J. *J. Chem. Phys.* **1985**, *82*, 284. (d) Hay, P.J.; Wadt, W.R. *J. Chem. Phys.* **1985**, *82*, 299.
5. (a) Scott, A.P.; Radom, L. *J. Phys. Chem.* **1996**, *100*, 16502. (b) Röder, J.C.; Meyer, F.; Hyla-Kryspin, I.; Winter, R.F.; Kaifer, E. *Chem. Eur. J.* **2003**, *9*, 2636. (c) Fox, M.A.; Roberts, R.L.; Khairul, W.M.; Hartl, F.; Low, P.J. *J. Organomet. Chem.* **2007**, *692*, 3277.

Table 1. Selected bond lengths (Å) and angles (°) for experimental and computed geometries

	Experimental [**3**]BF_4	Computed [**3-H**]$^+$
Fe-C(1)	1.828(3)	1.829
Fe(1)-P(1)	2.1803(8)	2.249
Fe(1)-P(2)	2.2033(7)	2.250
C(1)-C(2)	1.235(4)	1.257
C(2)-C(3)	1.348(4)	1.345
C(3)-N(1)	1.161(3)	1.185
N(1)-Re(1)	2.120(2)	2.096
Re(1)-N(2)	2.180(2)	2.151
Re(1)-N(3)	2.172(2)	2.151
P(1)-Fe(1)-P(2)	87.59(3)	86.91
P(1)-Fe(1)-C(1)	85.84(8)	88.32
P(2)-Fe(1)-C(1)	86.32(8)	90.45
Fe(1)-C(1)-C(2)	177.9(2)	179.7
C(1)-C(2)-C(3)	170.1(3)	179.5
C(2)-C(3)-N(1)	179.6(3)	179.2
C(3)-N(1)-Re(1)	169.2(2)	176.3
N(1)-Re(1)-N(2)	81.36(9)	85.69
N(2)-Re(1)-N(3)	74.61(8)	75.76
N(1)-Re(1)-C(10)	177.1(1)	177.8

Figure S1. Selected frontier orbitals for the cation [{Cp(dHpe)Fe}(μ-C≡CC≡N){Re(bpy)(CO)$_3$}]$^+$ [**3-H**]$^+$

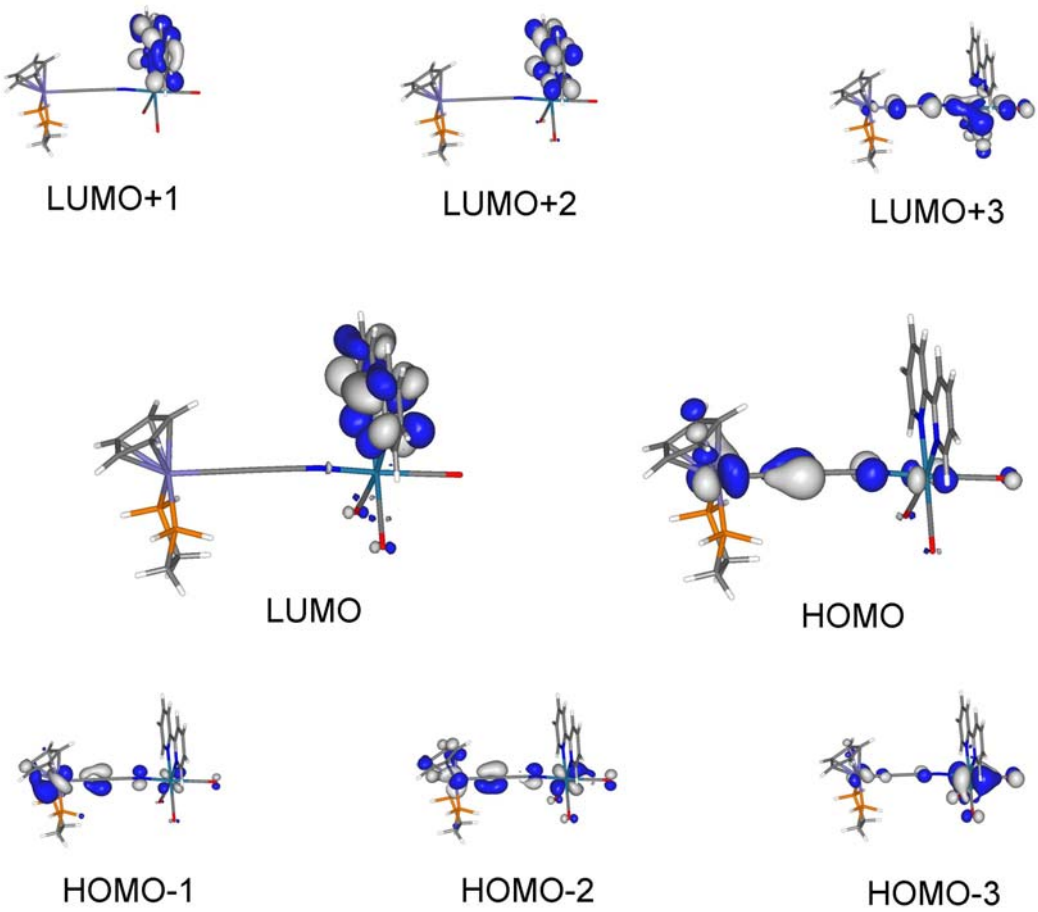

Table 2. Comparison of selected IR vibrational frequencies for [**3**]$^+$ and [**3**]$^{2+}$, calculated frequencies ([**3-H**]$^+$) and photoexcited [**3**]$^+$*.

	[**3-H**]$^+$	[**3**]$^+$	[**3**]$^+$* ‡	[**3**]$^{2+}$
ν(CN)	2204	2190	[a]	2210
ν(CO)	2016	2035	2011	2040
ν(CC)	1980	1970	[a]	2000
ν(CO)	1941	1930br	1908	1940br
ν(CO)(eq)	1934	1930br	1908	1940br

‡ Transient feature centroids become less accurate as time delay progression evolves and signal amplitude decreases.
[a] masked by bleach

Table 3. The orbital numbers, orbital type and composition (%) of selected orbitals for **[3-H]$^+$**

[3-H]$^+$

MO		eV	Cp	Fe	dppe	C(1)	C(2)	C(3)	N	Re	CO	$(CO)_2$	bpy
132	L+9	-2.45	1	7	6	2	1	0	1	21	19	41	2
131	L+8	-2.54	0	2	1	8	2	5	6	10	1	38	27
130	L+7	-2.56	0	1	0	3	1	2	2	3	0	13	74
129	L+6	-2.74	19	54	16	11	0	0	0	0	1	0	0
128	L+5	-3.26	23	51	21	1	0	1	1	1	1	1	0
127	L+4	-3.30	0	7	5	27	4	21	18	7	12	0	0
126	L+3	-3.37	0	6	5	19	2	17	12	15	12	11	0
125	L+2	-3.97	0	0	0	0	0	0	0	0	1	2	97
124	L+1	-4.14	0	0	0	0	0	0	0	1	0	1	98
123	LUMO	-5.11	0	0	0	0	0	0	0	2	0	3	94
122	HOMO	-8.17	7	40	3	3	16	0	8	15	4	3	1
121	H-1	-8.51	2	35	2	6	13	1	7	23	5	4	3
120	H-2	-8.79	17	54	6	4	1	1	1	12	2	2	2
119	H-3	-8.98	4	20	1	1	2	4	0	47	8	8	4
118	H-4	-9.15	0	1	0	0	0	0	0	70	0	27	1
117	H-5	-9.38	3	37	2	1	10	2	3	27	4	5	5
116	H-6	-10.02	47	39	4	4	3	0	1	1	0	0	0
115	H-7	-10.13	60	28	2	2	4	0	2	1	0	0	1
114	H-8	-10.30	1	1	0	1	0	0	0	0	0	0	96
113	H-9	-10.49	5	25	13	20	18	0	9	3	0	1	5
112	H-10	-10.85	18	31	6	20	13	0	8	2	0	1	3

Table 4 Excitation energies and oscillator strengths from TD-DFT computations (PBE1PBE//LANL2DZ/6-31G*) for **[3-H]**$^+$. See Table 3 for details on orbital numbers listed in the transitions.

Excitation energies and oscillator strengths for [**3-H**]$^+$:

Excited State 1: Singlet-A 2.2062 eV
561.97 nm f=0.0000
116 ->128 0.19742
117 ->128 0.11784
120 ->128 0.49138
121 ->128 -0.33509
122 ->129 0.16889

Excited State 2: Singlet-A 2.3057 eV
537.72 nm f=0.0016
119 ->123 0.18576
122 ->123 0.67813

Excited State 3: Singlet-A 2.3288 eV
532.39 nm f=0.0036
113 ->128 0.15867
119 ->128 -0.23377
122 ->128 0.54828

Excited State 4: Singlet-A 2.5365 eV
488.79 nm f=0.0001
112 ->128 -0.12412
113 ->129 0.11146
116 ->128 -0.17883
117 ->128 -0.30312
119 ->129 -0.16578
120 ->128 -0.18310
121 ->128 -0.22351
122 ->129 0.37564
122 ->130 -0.11893

Excited State 5: Singlet-A 2.6886 eV
461.15 nm f=0.0492
120 ->123 0.22629
121 ->123 0.64696

Excited State 6: Singlet-A 2.9088 eV
426.23 nm f=0.0071
112 ->129 0.13621
117 ->129 0.18717
120 ->129 -0.23654
121 ->129 0.49053
121 ->130 -0.15590
121 ->133 -0.10148

Excited State 7: Singlet-A 3.0252 eV
409.84 nm f=0.0016
119 ->123 0.66643
122 ->123 -0.19040

Excited State 8: Singlet-A 3.0321 eV
408.90 nm f=0.0001
118 ->123 0.67820
120 ->123 -0.11649

Excited State 9: Singlet-A 3.1176 eV
397.69 nm f=0.0095
117 ->123 -0.11278
118 ->123 0.12173
120 ->123 0.63748
121 ->123 -0.24149

Excited State 10: Singlet-A 3.1402 eV
394.83 nm f=0.0004
112 ->128 0.11470
117 ->128 0.25477
119 ->129 -0.13531
121 ->128 0.36353
122 ->129 0.33727
122 ->130 -0.10601

Excited State 11: Singlet-A 3.3303 eV
372.29 nm f=0.0017
119 ->124 0.14627
122 ->124 0.68346

Excited State 12: Singlet-A 3.4654 eV
357.77 nm f=0.0072
117 ->123 -0.22667
119 ->125 0.12407
121 ->127 0.10359
122 ->125 0.52823
122 ->126 -0.14773
122 ->127 -0.24369

Excited State 13: Singlet-A 3.4717 eV
357.13 nm f=0.0005
122 ->125 0.26471
122 ->127 0.59693

Excited State 14: Singlet-A 3.5194 eV
352.29 nm f=0.0248
116 ->129 0.16552
117 ->129 0.24711
120 ->129 0.29919
121 ->127 0.19603
122 ->125 -0.24853

122 ->126 -0.28012
122 ->127 0.12332

Excited State 15: Singlet-A 3.5785 eV 346.47 nm f=0.0284
117 ->123 0.59857
120 ->123 0.10498
121 ->124 0.19705
122 ->125 0.20869

Excited State 16: Singlet-A 3.6662 eV 338.18 nm f=0.0309
117 ->123 -0.16175
120 ->124 0.22060
121 ->124 0.61448
122 ->125 -0.13302

Excited State 17: Singlet-A 3.7592 eV 329.82 nm f=0.0073
117 ->125 -0.10373
120 ->125 0.23175
121 ->125 0.58383
121 ->126 -0.25700

Excited State 18: Singlet-A 3.7747 eV 328.46 nm f=0.0423
116 ->129 0.10665
117 ->129 0.15678
120 ->129 0.23731
121 ->127 -0.31595
122 ->126 0.45848

Excited State 19: Singlet-A 3.8531 eV 321.78 nm f=0.0017
120 ->125 0.11462
120 ->126 0.11031
121 ->125 0.24275
121 ->126 0.59462
121 ->131 -0.13585

Excited State 20: Singlet-A 4.0476 eV 306.32 nm f=0.0001
114 ->123 0.13170
119 ->124 0.66728
122 ->124 -0.15484

Excited State 21: Singlet-A 4.0834 eV 303.63 nm f=0.0030
118 ->124 -0.21644
120 ->124 0.60915
121 ->124 -0.25385

Excited State 22: Singlet-A 4.1355 eV 299.80 nm f=0.0004
117 ->124 -0.12556
118 ->124 0.65928
120 ->124 0.19797

Excited State 23: Singlet-A 4.2059 eV 294.79 nm f=0.0092
118 ->125 -0.25742
120 ->125 0.41636
120 ->126 -0.36988
120 ->127 -0.13063
121 ->125 -0.21162
121 ->127 0.10923
121 ->131 -0.10526

Excited State 24: Singlet-A 4.2240 eV 293.52 nm f=0.0197
118 ->125 0.57564
120 ->126 -0.23843
120 ->127 -0.17680
121 ->127 0.14266

Excited State 25: Singlet-A 4.2274 eV 293.29 nm f=0.0514
118 ->125 -0.12745
119 ->125 0.64829
122 ->125 -0.14222

Excited State 26: Singlet-A 4.2459 eV 292.01 nm f=0.0419
117 ->125 -0.10729
118 ->125 0.24334
119 ->125 0.11708
119 ->126 -0.13667
120 ->125 0.33177
120 ->127 0.36109
121 ->125 -0.14824
121 ->127 -0.23851
122 ->126 -0.13124
122 ->131 -0.12681

Synthetic details: A Schlenk flask was charged with [Fe(C≡CC≡N)(dppe)Cp] (50 mg, 0.088 mmol), $[Re(NCMe)(CO)_3(bpy)]PF_6$ (54 mg, 0.088 mmol) and thf (25 mL). The mixture was warmed to *ca*. 50°C and stirred for 48 h. The solvent was removed and the residue extracted with CH_2Cl_2. Hexane was added and the solution concentrated to give a yellow precipitate which was collected, washed with hexane, pentane and air-dried. Yield = 75 mg (75 %). Found C 49.86, H 3.43, N 3.63. $C_{47}H_{37}F_6FeN_3O_3P_3Re$ requires C 49.48, H 3.27, N 3.68. ^{1}H NMR ($CDCl_3$): δ 8.71 (dd, 4H, bpy), 8.29 (t, 2H, bpy), 7.56-7.09 (m, 22H, dppe + bpy), 4.30 (s, 5H, Cp), 2.37 (m, 4H, dppe). ^{31}P{H} NMR ($CDCl_3$): δ 102.6 (s, dppe), -143.0 (ht, J_{PF} = 713 Hz, $[PF_6]^-$). ^{13}C{H} NMR ($CDCl_3$): d 194.5 (s, 2 x CO), 190.3 (s, CO), 180.4 (t, J_{CP} 36 Hz, C_a), 155.8 (C1 bpy), 152.4 (C3 bpy), 141.2 (C5 bpy), 139.2, 134.5 (m, $C_{i,i'}$ dppe) 132.9, 131.4 (dd, $^2J_{CP}$,$^4J_{CP}$ ~ 5 Hz, $C_{o,o'}$ dppe), 130.3, 129.9 (s, $C_{p,p'}$ dppe), 128.5, 128.1 (dd, $^3J_{CP}$,$^5J_{CP}$ ~ 5 Hz, $C_{m,m'}$ dppe), 127.6, 125.3 (C2, C4 bpy), 104.5 (s, CN), 84.0 (s, C_b), 81.7 (s, Cp), 28.4 (m, CH_2 dppe). ^{19}F{H} NMR ($CDCl_3$) d -73.3 (d, J_{PF} 713 Hz, PF_6^-). MALDI-MS *m/z* 996, [**3**]$^+$. IR (CH_2Cl_2): ν(C≡N) 2188 cm^{-1}, ν(C≡C) 1970 cm^{-1}, ν(C≡O) 2035, 1930(br) cm^{-1}. The analogous compound [**3**]BF_4 was obtained from a similar reaction between [Fe(C≡CC≡N)(dppe)Cp] and $[Re(OTf)(CO)_3(bpy)]$, carried out in CH_2Cl_2 containing one molar equivalent of $NaBF_4$, and, in contrast to the PF_6^- salt, crystallized in a form suitable for X-ray diffraction by slow diffusion of methanol in a CH_2Cl_2 solution of the complex.

Crystallography

There is a disorder (1:1) of the ethylene bridge and two benzene rings at P(1) phosphorus atom, which corresponds to a racemic mixture of λ- and δ-conformers of [**3**]BF_4. The P(1) atom is also slightly disordered, however the attempts to model this disorder did not improved the refinement indicators. As a result the variation of observed P(1)-C bond lengths is rather high.